Calcolo (2017) 54:1379–1402
https://doi.org/10.1007/s10092-017-0232-5

An energy-preserving algorithm for nonlinear Hamiltonian wave equations with Neumann boundary conditions

Wei Shi[1] · **Kai Liu**[2] · **Xinyuan Wu**[3,4] · **Changying Liu**[5]

Received: 3 December 2016 / Accepted: 21 July 2017 / Published online: 2 August 2017

Abstract In this paper, a novel energy-preserving numerical scheme for nonlinear Hamiltonian wave equations with Neumann boundary conditions is proposed and analyzed based on the blend of spatial discretization by finite element method (FEM) and time discretization by Average Vector Field (AVF) approach. We first use the

The research was supported in part by the Natural Science Foundation of China under Grant 11501288 and 11671200, by the Specialized Research Foundation for the Doctoral Program of Higher Education under Grant 20100091110033, by the 985 Project at Nanjing University under Grant 9112020301, by A Project Funded by the Priority Academic Program Development of Jiangsu Higher Education Institutions, by the Natural Science Foundation of Jiangsu Province under Grant BK20150934, and by the Natural Science Foundation of the Jiangsu Higher Education Institutions under Grant 16KJB110010 and 14KJB110009.

✉ Changying Liu
chyliu88@gmail.com

Wei Shi
shuier628@163.com

Kai Liu
laukai520@163.com

Xinyuan Wu
xywu@nju.edu.cn

1 College of Mathematical Sciences, Nanjing Tech University, Nanjing, People's Republic of China

2 College of Applied Mathematics, Nanjing University of Finance and Economics, Nanjing, People's Republic of China

3 Department of Mathematics, Nanjing University, Nanjing, People's Republic of China

4 State Key Laboratory for Novel Software Technology at Nanjing University, Nanjing, People's Republic of China

5 College of Math and Statistics, Nanjing University of Information Science and Technology, Nanjing, People's Republic of China

finite element discretization in space, which leads to a system of Hamiltonian ODEs whose Hamiltonian can be thought of as the semi-discrete energy of the original continuous system. The stability of the semi-discrete finite element scheme is analyzed. We then apply the AVF approach to the Hamiltonian ODEs to yield a new and efficient fully discrete scheme, which can preserve exactly (machine precision) the semi-discrete energy. The blend of FEM and AVF approach derives a new and efficient numerical scheme for nonlinear Hamiltonian wave equations. The numerical results on a single-soliton problem and a sine-Gordon equation are presented to demonstrate the remarkable energy-preserving property of the proposed numerical scheme.

Keywords Nonlinear Hamiltonian wave equations · Energy-preserving schemes · Finite element discretization · Average vector field method

Mathematics Subject Classification 65L05 · 65L06

1 Introduction

Although a great number of conservative PDEs arises in pure and applied mathematics and in applied sciences, there has far less treatment of partial differential equations in the geometric integration literature than that of ordinary differential equations. Geometric integration for PDEs is still a relatively new area and there has not been much work in this research. The formulation of multi-symplectic methods [1] provides an approach to numerically computing conservative PDEs based on multi-symplectic geometry. Some conservative PDEs, for instance KdV equations, Schrödinger equations, wave equations can lend themselves to this approach. However, except for the multi-symplectic conservation law, Hamiltonian systems also have the energy and momentum conservation laws. Unfortunately, as Ge and Marsden [2] showed that exact energy conservation is, in general, not possible with a symplectic method. It is well-known that conservation law plays an important role in conservative PDEs, especially in the theory of solitons, and the energy conservation is an essential property in an elastic collision of two solitons.

In this paper, we consider a general class of nonlinear Hamiltonian systems of wave equations. Our main objective is to design an efficient energy-preserving discretization scheme using the blend of FEM and AVF approach for these kind of nonlinear Hamiltonian systems.

The system we are concerned with is the nonlinear Klein–Gordon equations of the form

$$\frac{\partial^2 u(x,t)}{\partial t^2} - \lambda \frac{\partial^2 u(x,t)}{\partial x^2} = f(u), \qquad (x,t) \in [x_L, x_R] \times [t_0, T], \tag{1}$$

where $u(x,t)$ represents the wave displacement at the position x and time t, and $f = -\nabla V(u)$ is the negative derivative of a smooth potential energy $V(u)$ with respect to u, and $\lambda > 0$.

The nonlinear wave equation (1) is subjected to the following initial conditions

$$\begin{cases} u(x,t_0) = \varphi_1(x), & t \geq t_0, \\ \dfrac{\partial u}{\partial t}(x,t_0) = \varphi_2(x), & t \geq t_0, \end{cases} \tag{2}$$

and Neumann boundary conditions

$$\frac{\partial u}{\partial x}(x_L,t) = \frac{\partial u}{\partial x}(x_R,t) = 0, \qquad t \geq t_0. \tag{3}$$

The Klein–Gordon equation (1) arises in a variety of application areas in science and engineering such as nonlinear optics, solid state physics and quantum field theory and has been investigated by many authors (see [3–6], for examples). This equation is the relativistic version of the Schrödinger equation [7,8]. It is of great importance in relativistic quantum mechanics, which is used to describe spinless particles. Such a problem appears naturally in the study of some nonlinear dynamical problems of mathematical physics, including radiation theory, general relativity, the scattering and stability of kinks, vortices, and other coherent structures. This equation has attracted much attention in studying solitons and condensed matter physics, in investigating the interaction of solitons in collisionless plasma and the recurrence of initial states, in lattice dynamics, and in examining the nonlinear wave equations. An important property of the Eq. (1) is the conservation of the *continuous energy* (see [9], for example):

$$E(t) = \frac{1}{2}\int_{x_L}^{x_R} \left(u_t^2 + \lambda u_x^2 + 2V(u)\right)dx \equiv \text{const}, \tag{4}$$

and thus the system is called "conservative". The energy conservation is an essential property in an elastic collision of two solitons.

When discretizing such a conservative system in space and time, it is a natural idea to design numerical schemes that preserve rigorously a discrete energy that is an equivalence of the continuous one, since they often yield physically correct results and numerical stability [10]. These kind of schemes are called "conservative schemes". In several areas of mechanics, the design of energy-conserving numerical methods has received some attention. For instance, in [11], authors presented several finite difference methods that preserve certain algebraic invariants for nonlinear Klein–Gordon equations based on finite difference calculus. In [12], the author developed the energy-preserving numerical methods for PDEs with variable coefficients by using the discrete variational derivative approach. For useful research on this topic, readers are referred to [13,14] and references therein.

Comparing with the traditional method of lines [15], our purpose in this paper is to design an energy-preserving numerical method based on the use of variational techniques (such as FEM) for the space semidiscretization since this approach ensures the conservation of a semi-discrete energy which is a discrete approximation of the original energy in a continuous conservative system of PDEs. The semidiscretization resulting from this kind of discretization in space suggests the form of second-order ordinary differential equations (ODEs) which can also be a Hamiltonian system of ODEs. In

such a way, the conserved PDEs can be converted into a system of Hamiltonian ODEs in time.

It is a quite natural idea to gain a full discrete scheme that can preserve the original energy as accurately as possible. To this end, it is very important to use an integrator that can preserve the semi-discrete energy exactly. Fortunately, the energy-preserving methods have been developed systematically in tackling with Hamiltonian ODEs (see [17–27], for examples). The Average vector Field (AVF) method was recently [16] shown to preserve the energy exactly for any vector field. It is related to discrete gradient methods [18] and amongst discrete gradient methods it is distinguished by its features of linear covariance, automatic preservation of linear symmetries, reversibility with respect to linear reversing symmetries, and often by its simplicity.

The facts mentioned above motivate us to consider the AVF method for the discretization of the converted system of Hamiltonian ODEs in time. Therefore, incorporating the finite element discretization in space with the AVF approach in time gives a novel energy-preserving numerical scheme for the Hamiltonian PDE (1). Most importantly, with this approach to dealing with conservative system of PDEs, the difference between the original energy and the numerical one occurs only in space discretization.

The paper is organized as follows. Section 2 is devoted to designing an energy-preserving discretization scheme for (1). We first use finite element discretization in space for (1) to obtain a Hamiltonian system of second-order ODEs and analyze the stability of the semi-discrete finite element scheme. We then apply the AVF method to the Hamiltonian system of ODEs. With this approach, a new energy-preserving numerical scheme for nonlinear Hamiltonian wave equations with Neumann boundary conditions is presented and its properties are discussed. In Sect. 3, we describe in detail the idea of the approach to the FEM discretization in space with a piecewise-linear polynomial basis. Numerical experiments on a single-soliton problem and a sine-Gordon equation are implemented and the numerical results show the favourable conservative property of the new scheme in Sect. 4. Sect. 5 is concerned with conclusions.

2 An energy-preserving numerical scheme based on FEM and AVF

In this section, combining finite element method with the AVF approach, we present an energy-preserving numerical scheme for the Hamiltonian PDEs (1).

2.1 Spatial semidiscretization: semi-discrete finite element formulation

We first discretize the spatial derivative by using standard continuous finite elements while leaving time continuous.

2.1.1 Variational formulation

The weak formulation of the underlying problem (1) over (x_L, x_R) is given by [28]

$$\int_{x_L}^{x_R} \left(u_{tt} v - \lambda u_{xx} v\right) dx = \int_{x_L}^{x_R} f(u) v dx, \tag{5}$$

where $v \in S^1 = H^1([x_L, x_R]) \times (t \geq t_0)$ is an arbitrary test function and may be viewed as the variation in $u \in S^1$. After applying the divergence theorem to the second derivative terms u_{xx}, we arrive at the following system of equations

$$\int_{x_L}^{x_R} u_{tt} v dx + \lambda \int_{x_L}^{x_R} u_x v_x dx - u_x v \,|_{x_L}^{x_R} = \int_{x_L}^{x_R} f(u) v dx. \tag{6}$$

In order to use a variational formulation, we first introduce the bilinear form $a : H^1([x_L, x_R]) \times H^1([x_L, x_R]) \to \mathcal{R}$:

$$a(u, v) = \int_{x_L}^{x_R} u_x v_x dx, \qquad \forall u, v \in H^1([x_L, x_R]).$$

Here, $a(\cdot, \cdot)$ is symmetric and bounded on $H^1([x_L, x_R]) \times H^1([x_L, x_R])$, satisfying

$$|a(u, v)| \leq \beta \, \|u\|_{H^1} \, \|v\|_{H^1}, \quad \forall u, v \in H^1([x_L, x_R]).$$

The Neumann boundary condition (3) gives the following variational formulation

$$(u_{tt}, v) + \lambda a(u, v) = (f, v), \tag{7}$$

where

$$(u_{tt}, v) = \int_{x_L}^{x_R} u_{tt} v dx, \quad (f(u), v) = \int_{x_L}^{x_R} f(u) v dx.$$

In what follows, it is required to find $u \in S^1$ satisfying Eq. (7) with the initial condition

$$u(x, t_0) = \varphi_1(x), \; u_t(x, t_0) = \varphi_2(x).$$

2.1.2 Finite element model

Let

$$h = \frac{x_R - x_L}{N - 1}$$

be the stepsize of spatial direction and discretize the interval $[x_L, x_R]$ with the spatial grid points $x_i = x_L + (i - 1)h, \; i = 1, 2, \ldots, N$. We introduce a finite-dimensional subspace S_h^1 of H^1 with the basis functions $\phi_i, \; i = 1, \ldots, N$, namely,

$$S_h^1 = \text{span}\{\phi_1, \phi_2, \ldots, \phi_N\},$$

and choose an approximation $\hat{u}$ of u in S_h^1 having the form

$$\hat{u}(x, t) = \sum_{j=1}^{N} w_j(t) \phi_j(x), \tag{8}$$

where the coefficients $w_j, \; j = 1, 2, \ldots, N$ depend on t.

The finite element problem is to determine $\hat{u}(x,t)$ such that

$$(\hat{u}_{tt},\phi_i)+\lambda a(\hat{u},\phi_i)=(f(\hat{u}),\phi_i), \tag{9}$$

subject to the initial conditions

$$(\hat{u}(x,t_0),\phi_i(x))=(\varphi_1(x),\phi_i(x)),\qquad (\hat{u}_t(x,t_0),\phi_i(x))=(\varphi_2(x),\phi_i(x)). \tag{10}$$

The i-th equation of the system is

$$\int_{x_L}^{x_R}\phi_i\left(\sum_{j=1}^{N}\frac{dw_j^2}{dt^2}\phi_j\right)dx+\int_{x_L}^{x_R}\lambda\frac{d\phi_i}{dx}\left(\sum_{j=1}^{N}\frac{d\phi_j}{dx}w_j\right)dx=\int_{x_L}^{x_R}f\phi_i dx, \tag{11}$$

i.e.,

$$\sum_{j=1}^{N}\left[\left(\int_{x_L}^{x_R}\phi_i\phi_j dx\right)\frac{dw_j^2}{dt^2}+\lambda\left(\int_{x_L}^{x_R}\frac{d\phi_i}{dx}\frac{d\phi_j}{dx}dx\right)w_j\right]=\int_{x_L}^{x_R}f\phi_i dx. \tag{12}$$

The Eq. (12) can be written in the matrix form

$$AU''(t)+BU(t)=F(U), \tag{13}$$

where

$$U(t)=(w_1(t),w_2(t),\ldots,w_N(t))^{\mathsf{T}},$$

$A, B\in\mathcal{R}^{N\times N}$ with

$$A_{ij}=(\phi_i,\phi_j)=\int_{x_L}^{x_R}\phi_i\phi_j dx,\quad i,j=1,\ldots,N,$$
$$B_{ij}=\lambda(\phi_i',\phi_j')=\lambda\int_{x_L}^{x_R}\frac{d\phi_i}{dx}\frac{d\phi_j}{dx}dx,\quad i,j=1,\ldots,N,$$

and $F\in\mathcal{R}^N$ with

$$F_i=(f,\phi_i)=\int_{x_L}^{x_R}f\phi_i dx,\quad i=1,\ldots,N.$$

In order to solve the system of ODEs (13), we need to determine the initial values $U(t_0)$ and $U'(t_0)$ from (10), i.e.,

$$AU(t_0)=\begin{pmatrix}\int_{x_L}^{x_R}\varphi_1\phi_1 dx\\ \vdots\\ \int_{x_L}^{x_R}\varphi_1\phi_N dx\end{pmatrix},\qquad AU'(t_0)=\begin{pmatrix}\int_{x_L}^{x_R}\varphi_2\phi_1 dx\\ \vdots\\ \int_{x_L}^{x_R}\varphi_2\phi_N dx\end{pmatrix}. \tag{14}$$

It can be observed that both A and B are symmetric matrices. The mass matrix A is positive definite, and the stiffness matrix B is in general, positive semidefinite. F can be written as $F(U) = -\nabla_U \overline{V}(U)$ with

$$\overline{V}(U) = \int_{x_L}^{x_R} V(\hat{u})dx = \int_{x_L}^{x_R} V\left(\sum_{j=1}^{N} w_j \phi_j(x)\right) dx = \int_{x_L}^{x_R} V(\Phi(x)^\intercal U)dx,$$

where $\Phi(x) = (\phi_1(x), \phi_2(x), \ldots, \phi_N(x))^\intercal$. Thus, the system (13) is a Hamiltonian system on time t with the Hamiltonian

$$H(p, q) = \frac{1}{2} p^\intercal A^{-1} p + \frac{1}{2} q^\intercal B q + \overline{V}(q), \tag{15}$$

where $p = AU'$ and $q = U$. In other words, the system (13) has a conservative energy

$$H(p, q) = H(AU', U) = \frac{1}{2} U'^\intercal A U' + \frac{1}{2} U^\intercal B U + \overline{V}(U). \tag{16}$$

For simplicity, we denote it by $H(U', U)$.

Remark 1 It should be noted that the zero Neumann boundary condition is imposed for the wave equation throughout the paper. The reason is that we need to guarantee the resulting system of ODEs is Hamiltonian after FEM semi-discretization in space so that the AVF methods could be used in temporal direction. It does not always hold for other types of boundary conditions. However, one can verify that the periodic boundary condition and zero Dirichlet boundary condition satisfy the demand. And the treatment in the paper is applicable in these two cases.

From the existence theory of ordinary differential equations, the problem has a unique solution on $[t_0, t_{end}]$ if the function $f(t, y)$ is continuous in its first variable and satisfies a Lipschitz condition in its second variable (see Butcher [29]). Therefore, the existence and uniqueness of a local solution U of (13) is a direct consequence.

Moreover, we have the following important result on the preservation of semidiscrete energy.

Theorem 1 *The scheme* (9)*, or equivalently* (13)*, preserves a semidiscrete energy, namely, the solution U of the scheme satisfies:*

$$\frac{d}{dt}\tilde{E}(t) = 0,$$

with

$$\tilde{E}(t) = \frac{1}{2} \int_{x_L}^{x_R} \left(\hat{u}_t^2 + \lambda \hat{u}_x^2 + 2V(\hat{u})\right) dx. \tag{17}$$

Proof This property comes directly from the variational formulation. With $v(x) = \partial_t \hat{u}(x, t)$, we then have

$$(\hat{u}_{tt}, \hat{u}_t) + \lambda a(\hat{u}, \hat{u}_t) = (f(\hat{u}), \hat{u}_t), \tag{18}$$

i.e.,

$$\int_{x_L}^{x_R} \hat{u}_{tt}\hat{u}_t dx + \lambda \int_{x_L}^{x_R} \hat{u}_x \hat{u}_{tx} dx = \int_{x_L}^{x_R} f(\hat{u})\hat{u}_t dx. \tag{19}$$

It can be rewritten as

$$\int_{x_L}^{x_R} \left[\frac{1}{2}\frac{\partial}{\partial t}(\hat{u}_t^2) + \frac{\lambda}{2}\frac{\partial}{\partial t}(\hat{u}_x^2) + \frac{\partial}{\partial t} V(\hat{u}) \right] dx = 0, \tag{20}$$

which leads to the result. □

Theorem 1 allows us to show that the solution $\hat{u}(x,t)$ is global in time and provides H^1 stability estimates, which is stated by the following theorem.

Theorem 2 *Assume the function $V(\cdot)$ is positive and $\hat{u}(x,t)$ is the solution of the finite element problem (9)–(10). Then, the semi-discrete finite element scheme is stable in the H^1 norm with respect to the initial value, namely, there exist a constant $C \geq 0$ such that*

$$\left\|\hat{u}(\cdot,t)\right\|_{H^1}^2 \leq C\tilde{E}(t_0) + 2\|\varphi_1\|^2.$$

Proof According to Theorem 1, we have

$$\left\|\hat{u}_t(\cdot,t)\right\|^2 + \lambda \left\|\hat{u}_x(\cdot,t)\right\|^2 + 2\int_{x_L}^{x_R} V(\hat{u}) dx = 2\tilde{E}(t_0),$$

and it follows from $V(\hat{u}) > 0$ that

$$\left\|\hat{u}_t(\cdot,t)\right\|^2 \leq 2\tilde{E}(t_0), \quad \left\|\hat{u}_x(\cdot,t)\right\|^2 \leq \frac{2}{\lambda}\tilde{E}(t_0).$$

For $\forall t \geq t_0$, Cauchy–Schwarz inequality gives

$$\begin{aligned}\hat{u}^2(x,t) &\leq 2\hat{u}^2(x,t_0) + 2\left(\int_{t_0}^{t} \hat{u}_t(x,s) ds\right)^2 \\ &\leq 2\hat{u}^2(x,t_0) + 2(t-t_0)\left(\int_{t_0}^{t} \hat{u}_t^2(x,s) ds\right).\end{aligned}$$

Therefore,

$$\left\|\hat{u}(\cdot,t)\right\|^2 \leq 2\left\|\hat{u}(\cdot,t_0)\right\|^2 + 2(t-t_0)\int_{t_0}^{t} \left\|\hat{u}_t(\cdot,s)\right\|^2 ds,$$

and this yields

$$\left\|\hat{u}(\cdot,t)\right\|_{H^1}^2 = \left\|\hat{u}(\cdot,t)\right\|^2 + \left\|\hat{u}_x(\cdot,t)\right\|^2 \leq C\tilde{E}(t_0) + 2\|\varphi_1\|^2.$$

Remark 2 The function V here is assumed to be positive. Since the function V is only used through its gradient, any $V + c$ can fit for the equations, with $c \in R^+$.

As a matter of fact, $\hat{E}(t)$ is exactly the Hamiltonian of the ODEs (13), which can be verified by substituting the expression (8) of $\hat{u}(x,t)$ into (17).

2.2 Time discretization: average vector field method

In this subsection, we consider the time discretization of the ODEs (13) and investigate how to find a scheme that can preserve rigorously the semi-discrete energy.

2.2.1 The formulation of the AVF method for the ODEs (13)

The following theorem gives the AVF method to preserve the semi-discrete energy (16), or equivalently, (17), for the Hamiltonian system (13).

Theorem 3 *By the following AVF formula*

$$\begin{aligned} AU_{n+1} &= AU_n + \tau AU'_n + \frac{1}{2}\tau^2 \int_0^1 g((1-\xi)U_n + \xi U_{n+1})d\xi, \\ AU'_{n+1} &= AU'_n + \tau \int_0^1 g((1-\xi)U_n + \xi U_{n+1})d\xi \end{aligned} \tag{21}$$

with $g(U) = -BU - \nabla_U \overline{V}(U)$ *and* τ *the time stepsize, the energy of the Hamiltonian system* (13) *is conserved, i.e.,*

$$H(U'_{n+1}, U_{n+1}) = H(U'_n, U_n).$$

Proof Let

$$I_g = \int_0^1 g((1-\xi)U_n + \xi U_{n+1})d\xi.$$

We calculate

$$H\left(U'_{n+1}, U_{n+1}\right) = \frac{1}{2}U'^{\intercal}_{n+1}AU_{n+1} + \frac{1}{2}U^{\intercal}_{n+1}BU_{n+1} + \overline{V}(U_{n+1}). \tag{22}$$

Inserting (21) into (22) and keeping A and B are symmetric matrices in mind gives

$$\begin{aligned} H\left(U'_{n+1}, U_{n+1}\right) = &\frac{1}{2}U'^{\intercal}_n AU'_n + \frac{1}{2}U^{\intercal}_n BU_n + \tau U'^{\intercal}_n I_g + \tau U^{\intercal}_n BU'_n \\ &+ \frac{1}{2}\tau^2 I^{\intercal}_g A^{-1} I_g + \frac{1}{2}\tau^2 U^{\intercal}_n BA^{-1} I_g + \frac{1}{2}\tau^2 U'^{\intercal}_n BU'_n \\ &+ \frac{1}{2}\tau^3 U'^{\intercal}_n BA^{-1} I_g + \frac{1}{8}\tau^4 I^{\intercal}_g A^{-1} BA^{-1} I_g + \overline{V}(U_{n+1}). \end{aligned} \tag{23}$$

On the other hand, we have

$$H(U_n', U_n) = \frac{1}{2} U_n'^{\intercal} A U_n' + \frac{1}{2} U_n^{\intercal} B U_n + \overline{V}(U_n), \tag{24}$$

and

$$\begin{aligned}
&\overline{V}(U_n) - \overline{V}(U_{n+1}) \\
&= -\int_0^1 d\overline{V}\left((1-\xi)U_n + \xi U_{n+1}\right) \\
&= -\int_0^1 (U_{n+1} - U_n)^{\intercal} \nabla_U \overline{V}\left((1-\xi)U_n + \xi U_{n+1}\right) d\xi \\
&= (U_{n+1} - U_n)^{\intercal} \int_0^1 \Big(g\left((1-\xi)U_n + \xi U_{n+1}\right) \\
&\quad + B\left((1-\xi)U_n + \xi U_{n+1}\right)\Big) d\xi \\
&= (U_{n+1} - U_n)^{\intercal} I_g + (U_{n+1} - U_n)^{\intercal} B \frac{U_n + U_{n+1}}{2}.
\end{aligned} \tag{25}$$

Inserting (21) into (25) and comparing with (22) and (24) yield the result. □

Remark 3 It can be verified that this scheme is reversible in time.

Remark 4 Since $\overline{V}(U) = \int_{x_L}^{x_R} V(\Phi(x)^{\intercal} U) dx$, at first sight, there is a double integral in I_g and the approximation to it is quite complicated. However, taking into account the special structure of $\overline{V}(U)$ and exchanging the order of integrals, we can simplify the evaluation of I_g. The details are described below:

$$\begin{aligned}
&\int_0^1 g((1-\xi)U_n + \xi U_{n+1}) d\xi \\
&= -\frac{1}{2} B(U_{n+1} + U_n) - \int_0^1 \nabla_U \overline{V}((1-\xi)U_n + \xi U_{n+1}) d\xi \\
&= -\frac{1}{2} B(U_{n+1} + U_n) \\
&\quad - \int_0^1 \nabla_U \left(\int_{x_L}^{x_R} V\Big(\Phi(x)^{\intercal}((1-\xi)U_n + \xi U_{n+1})\Big) dx \right) d\xi \\
&= -\frac{1}{2} B(U_{n+1} + U_n) \\
&\quad - \int_{x_L}^{x_R} \Phi(x) \frac{V(\Phi(x)^{\intercal} U_{n+1}) - V(\Phi(x)^{\intercal} U_n)}{\Phi(x)^{\intercal} U_{n+1} - \Phi(x)^{\intercal} U_n} dx.
\end{aligned} \tag{26}$$

In practice, usually the integrals in (14) and (26) can not be evaluated exactly. Therefore, suitable quadratures should be used to approximate the integrals.

Up to now, we have obtained a full discretization for the Hamiltonian PDEs (1) by first semidiscretizing the equations using finite element methods and then applying

the AVF method to resulted ODEs. Noticing that the AVF method is of order 2, we assume that the finite element method used in spatial direction is of order $p \geq 2$. If the order of the quadrature formulae used in the approximation of the integrals mentioned above is greater that p, then the order of the full discretization would be $\mathcal{O}(h^p + \tau^2)$.

Remark 5 Denote the numerical solution and its derivative at time step t_n of the wave equation as $\hat{u}^n(x) = \sum_{j=1}^{N} w_j^n \phi_j(x)$, and $\hat{u}'^n(x) = \sum_{j=1}^{N} w_j'^n \phi_j(x)$, where $U_n = \left(w_1^n, w_2^n, \ldots, w_N^n\right)^{\mathsf{T}}$, $U_n' = \left(w_1'^n, w_2'^n, \ldots, w_N'^n\right)^{\mathsf{T}}$ is the numerical solution of resulting system ODEs by AVF method. By Theorem 3, we have

$$H\left(U_{n+1}', U_{n+1}\right) = H\left(U_n', U_n\right),$$

where $H(U_n', U_n)$ is exactly $\hat{E}(t_n)$ as shown in previous section. Therefore, we have

$$\begin{aligned} &\frac{1}{2}\int_{x_L}^{x_R}\left(\left(\hat{u}'^{n+1}(x)\right)^2 + \lambda\left(\hat{u}_x^{n+1}(x)\right)^2 + 2V\left(\hat{u}^{n+1}(x)\right)\right)dx \\ &\quad = \frac{1}{2}\int_{x_L}^{x_R}\left((\hat{u}'^{n}(x))^2 + \lambda(\hat{u}_x^n(x))^2 + 2V(\hat{u}^n(x))\right)dx. \end{aligned}$$

The numerical stability of the full discretization can be attained by a similar discussion as Theorem 1.

2.2.2 *Stability property of the AVF method for ODEs*

In this subsection, we consider the stability property of the AVF formula (21).

For system (13), the corresponding multidimensional linear equation is

$$Ay'' + By = 0, \tag{27}$$

since A is a symmetric and positive definite matrix and B is a symmetric and positive semi-definite matrix, there exists a nonsingular matrix P and a positive semi-definite diagonal matrix Λ_B so that A and B can be expressed as

$$A = P^T I P, \ B = P^T \Lambda_B P,$$

where I is the identity matrix sharing the same order as A.

With the variable substitution $z(t) = Py(t)$, the Eq. (27) is identical to a transformed equation

$$z'' + \Lambda_B z = 0. \tag{28}$$

Therefore, as described in [30], we use the following scalar second-order homogeneous linear equation as test model

$$y''(t) = -\lambda^2 y(t), \quad \text{with } \lambda \geq 0. \tag{29}$$

Applying the AVF formula (21) to (29) yields

$$\begin{cases} y_{n+1} = y_n + \tau y'_n - \dfrac{1}{4}\eta^2(y_{n+1} + y_n), \quad \eta = \tau\lambda, \\ \tau y'_{n+1} = \tau y'_n - \dfrac{1}{2}\eta^2(y_{n+1} + y_n). \end{cases} \tag{30}$$

Thus, the numerical solution delivers the recursion

$$\begin{pmatrix} y_{n+1} \\ \tau y'_{n+1} \end{pmatrix} = S(\eta) \begin{pmatrix} y_n \\ \tau y'_n \end{pmatrix},$$

where the stability matrix $S(\eta)$ is determined by

$$S(\eta) = \frac{1}{4+\eta^2} \begin{pmatrix} 4-\eta^2 & 4 \\ -4\eta^2 & 4-\eta^2 \end{pmatrix} \tag{31}$$

The behavior of the numerical solution depends on the eigenvalues of the stability matrix $S(\eta)$, and the stability properties of the AVF formula (21) are characterized by the spectral radius $\rho(S)$. The interval of stability, interval of periodicity, A-stability, and P-stability are defined as follows (see, e.g., [30]):

- $I_s = \{\eta > 0 |\ \rho(S) < 1\}$ is called the *interval of stability*.
- $I_p = \{\eta > 0 |\ \rho(S) = 1 \text{ and } \mathrm{tr}(S)^2 < 4\det(S)\}$ is called the *interval of periodicity*.
- If $I_s = (0, \infty)$, the method is called *A-stable*.
- If $I_p = (0, \infty)$, the method is called *P-stable*.

The spectral radius $\rho(S)$ is determined by the roots of the characteristic equation

$$\xi^2 - \mathrm{tr}(S)\xi + \det(S) = 0.$$

By solving the characteristic equation, we obtain that $\mathrm{tr}(S) = \frac{8-2\eta^2}{4+\eta^2}$, $\det(S) = 1$, $\rho(S) = 1$. Therefore, the AVF method (21) is P-stable.

Remark 6 The methodology of derivation of energy-preserving scheme in the paper can be generalized to higher dimensional case. The mass matrix A and the stiffness matrix B can be easily obtained once a certain finite element is assigned. The only issue that should be carefully addressed is the computation of $F(U)$ in (13), since it involves a series of multiple integrals. In the following, we consider the two-dimensional case with rectangle domain $[x_L, x_R] \times [y_L, y_R]$. The domain is meshed with the spatial grid points $(x_i, y_j) = (x_L + (i-1)h, y_L + (j-1)h)$, $i = 1, 2, \ldots, N_x$, $j = 1, 2, \ldots, N_y$. A relatively simple choice of the basis functions would be $\{\phi_i(x)\phi_j(y),\ i = 1, 2, \ldots, N_x, j = 1, 2, \ldots, N_y\}$, where $\phi_i(x)$ is defined similarly as that shown in Fig. 1. In this case, after some tedious manipulation, the general entry of $F(U)$ can be simplified as follows. Similar to the one-dimensional case, these double integrals could be approximated by suitable two-dimensional quadrature formulae.

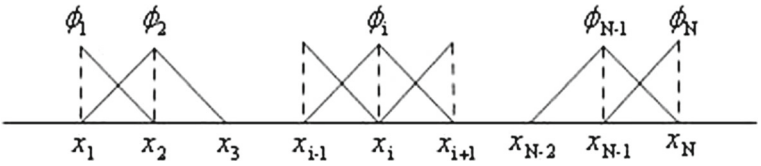

Fig. 1 Piecewise linear polynomial basis

3 Illustration by a selected piecewise-linear polynomial basis

We employ the following piecewise-linear polynomial basis as shown in Fig. 1, which gives a second-order semidiscretization in spatial direction.

Using this basis, we obtain

$$\phi_1(x) = \begin{cases} \frac{x_2 - x}{x_2 - x_1}, & x_1 < x \le x_2; \\ 0, & \text{otherwise}, \end{cases}$$

$$\phi_i(x) = \begin{cases} \frac{x - x_{i-1}}{x_i - x_{i-1}}, & x_{i-1} < x \le x_i; \\ \frac{x_{i+1} - x}{x_{i+1} - x_i}, & x_i < x \le x_{i+1} \quad i = 2, \ldots, N-1; \\ 0, & \text{otherwise}. \end{cases}$$

$$\phi_N(x) = \begin{cases} \frac{x - x_{N-1}}{x_N - x_{N-1}}, & x_{N-1} < x \le x_N; \\ 0, & \text{otherwise}, \end{cases}$$

and therefore,

$$A = \frac{h}{6} \begin{pmatrix} 2 & 1 & & & \\ 1 & 4 & 1 & & \\ & \ddots & \ddots & \ddots & \\ & & 1 & 4 & 1 \\ & & & 1 & 2 \end{pmatrix}, \; B = \frac{\lambda}{h} \begin{pmatrix} 1 & -1 & & & \\ -1 & 2 & -1 & & \\ & \ddots & \ddots & \ddots & \\ & & -1 & 2 & -1 \\ & & & -1 & 1 \end{pmatrix}. \tag{32}$$

We now deal with the following integral which appears in Eq. (26)

$$\int_{x_L}^{x_R} \Phi(x) \frac{V(\Phi(x)^\intercal U_{n+1}) - V(\Phi(x)^\intercal U_n)}{\Phi(x)^\intercal U_{n+1} - \Phi(x)^\intercal U_n} dx.$$

In the context of finite elements, by decomposing the global integral as the sum of integrals along the segments of the finite element mesh, we calculate every entry separately as follows

$$
\begin{aligned}
&\int_{x_L}^{x_R} \phi_1(x) \frac{V(\Phi(x)^\intercal U_{n+1}) - V(\Phi(x)^\intercal U_n)}{\Phi(x)^\intercal U_{n+1} - \Phi(x)^\intercal U_n} dx \\
&= \int_{x_1}^{x_2} \phi_1(x) \frac{V\left(\phi_1(x) w_1^{n+1} + \phi_2(x) w_2^{n+1}\right) - V\left(\phi_1(x) w_1^n + \phi_2(x) w_2^n\right)}{\phi_1(x)(w_1^{n+1} - w_1^n) + \phi_2(x)(w_2^{n+1} - w_2^n)} dx \\
&= \int_{x_1}^{x_2} \frac{x_2 - x}{h} \frac{V\left(\frac{x_2-x}{h} w_1^{n+1} + \frac{x-x_1}{h} w_2^{n+1}\right) - V\left(\frac{x_2-x}{h} w_1^n + \frac{x-x_1}{h} w_2^n\right)}{\frac{x_2-x}{h}(w_1^{n+1} - w_1^n) + \frac{x-x_1}{h}(w_2^{n+1} - w_2^n)} dx \\
&\overset{\xi = \frac{x-x_1}{h}}{=\!=\!=} h \int_0^1 (1-\xi) \frac{V\left((1-\xi) w_1^{n+1} + \xi w_2^{n+1}\right) - V\left((1-\xi) w_1^n + \xi w_2^n\right)}{(1-\xi)(w_1^{n+1} - w_1^n) + \xi(w_2^{n+1} - w_2^n)} d\xi \\
&= h \int_0^1 (1-\xi) \frac{V\left((1-\xi) w_1^{n+1} + \xi w_2^{n+1}\right) - V\left((1-\xi) w_1^n + \xi w_2^n\right)}{\left((1-\xi) w_1^{n+1} + \xi w_2^{n+1}\right) + \left((1-\xi) w_1^n + \xi w_2^n\right)} d\xi.
\end{aligned}
$$

Similarly, for $i = 2, \ldots, N-1$, we obtain

$$
\begin{aligned}
&\int_{x_L}^{x_R} \phi_i(x) \frac{V(\Phi(x)^\intercal U_{n+1}) - V(\Phi(x)^\intercal U_n)}{\Phi(x)^\intercal U_{n+1} - \Phi(x)^\intercal U_n} dx \\
&= \int_{x_{i-1}}^{x_i} \phi_i(x) \frac{V\left(\phi_{i-1}(x) w_{i-1}^{n+1} + \phi_i(x) w_i^{n+1}\right) - V\left(\phi_{i-1}(x) w_{i-1}^n + \phi_i(x) w_i^n\right)}{\phi_{i-1}(x)(w_{i-1}^{n+1} - w_{i-1}^n) + \phi_i(x)(w_i^{n+1} - w_i^n)} dx \\
&\quad + \int_{x_i}^{x_{i+1}} \phi_i(x) \frac{V\left(\phi_i(x) w_i^{n+1} + \phi_{i+1}(x) w_{i+1}^{n+1}\right) - V\left(\phi_i(x) w_i^n + \phi_{i+1}(x) w_{i+1}^n\right)}{\phi_i(x)(w_i^{n+1} - w_i^n) + \phi_{i+1}(x)(w_{i+1}^{n+1} - w_{i+1}^n)} dx \\
&= h \int_0^1 \xi \frac{V\left((1-\xi) w_{i-1}^{n+1} + \xi w_i^{n+1}\right) - V\left((1-\xi) w_{i-1}^n + \xi w_i^n\right)}{\left((1-\xi) w_{i-1}^{n+1} + \xi w_i^{n+1}\right) + \left((1-\xi) w_{i-1}^n + \xi w_i^n\right)} d\xi \\
&\quad + h \int_0^1 (1-\xi) \frac{V\left((1-\xi) w_i^{n+1} + \xi w_{i+1}^{n+1}\right) - V\left((1-\xi) w_i^n + \xi w_{i+1}^n\right)}{\left((1-\xi) w_i^{n+1} + \xi w_{i+1}^{n+1}\right) + \left((1-\xi) w_i^n + \xi w_{i+1}^n\right)} d\xi,
\end{aligned}
$$

and

$$
\begin{aligned}
&\int_{x_L}^{x_R} \phi_N(x) \frac{V(\Phi(x)^\intercal U_{n+1}) - V(\Phi(x)^\intercal U_n)}{\Phi(x)^\intercal U_{n+1} - \Phi(x)^\intercal U_n} dx \\
&= \int_{x_N-1}^{x_N} \phi_N(x) \frac{V\left(\phi_{N-1}(x) w_{N-1}^{n+1} + \phi_N(x) w_N^{n+1}\right) - V\left(\phi_{N-1}(x) w_{N-1}^n + \phi_N(x) w_N^n\right)}{\phi_{N-1}(x)(w_{N-1}^{n+1} - w_{N-1}^n) + \phi_N(x)(w_N^{n+1} - w_N^n)} dx \\
&= h \int_0^1 \xi \frac{V\left((1-\xi) w_{N-1}^{n+1} + \xi w_N^{n+1}\right) - V\left((1-\xi) w_{N-1}^n + \xi w_N^n\right)}{\left((1-\xi) w_{N-1}^{n+1} + \xi w_N^{n+1}\right) + \left((1-\xi) w_{N-1}^n + \xi w_N^n\right)} d\xi.
\end{aligned}
$$

The integrals in the right-hand side of the initial conditions (14) can be dealt with in a similar way and then we yield

$$AU(t_0) = h\int_0^1 \Psi_1(\xi)d\xi, \tag{33}$$

and

$$AU'(t_0) = h\int_0^1 \Psi_2(\xi)d\xi, \tag{34}$$

where

$$\Psi_1(\xi) = \begin{pmatrix} \varphi_1(x_2 - h\xi)\xi \\ \varphi_1(x_1 + h\xi)\xi + \varphi_1(x_3 - h\xi)\xi \\ \vdots \\ \varphi_1(x_{i-1} + h\xi)\xi + \varphi_1(x_{i+1} - h\xi)\xi \\ \vdots \\ \varphi_1(x_{N-2} + h\xi)\xi + \varphi_1(x_N - h\xi)\xi \\ \varphi_1(x_{N-1} + h\xi)\xi \end{pmatrix}$$

and

$$\Psi_2(\xi) = \begin{pmatrix} \varphi_2(x_2 - h\xi)\xi \\ \varphi_2(x_1 + h\xi)\xi + \varphi_2(x_3 - h\xi)\xi \\ \vdots \\ \varphi_2(x_{i-1} + h\xi)\xi + \varphi_2(x_{i+1} - h\xi)\xi \\ \vdots \\ \varphi_2(x_{N-2} + h\xi)\xi + \varphi_2(x_N - h\xi)\xi \\ \varphi_2(x_{N-1} + h\xi)\xi \end{pmatrix}$$

Note that A is a tridiagonal matrix, the Thomas method can be used to determine the initial values and in the implicit iteration of every step of the numerical scheme. Since all the integral intervals are rescaled to $[0, 1]$, we approximate the integrals by a quadrature with $(b_i, c_i),\ i = 1, \ldots, s$ the weights and nodes of the quadrature rule on $[0, 1]$. As an example, here and in the following, we choose the two-point Gauss–Legendre's rule with

$$b_1 = b_2 = \frac{1}{2},\ c_1 = \frac{3 - \sqrt{3}}{6},\ c_2 = \frac{3 + \sqrt{3}}{6},$$

and four-point Gauss–Legendre's rule with

$$b_1 = b_4 = \frac{18-\sqrt{30}}{36}, \quad b_2 = b_3 = \frac{18+\sqrt{30}}{36},$$
$$c_1 = \frac{1-\sqrt{\frac{15+2\sqrt{30}}{35}}}{2}, \quad c_2 = \frac{1-\sqrt{\frac{15-2\sqrt{30}}{35}}}{2},$$
$$c_3 = \frac{1+\sqrt{\frac{15-2\sqrt{30}}{35}}}{2}, \quad c_4 = \frac{1+\sqrt{\frac{15+2\sqrt{30}}{35}}}{2}.$$

Remark 7 In this section, we illustrate the new energy-preserving scheme by using a piecewise-linear polynomial basis in space. It should be noted that other high-degree piecewise polynomial basis could be used to give a high-order scheme. The only difference between the piecewise-linear case and others is the construction of the matrices A and B, which only needs more tedious computation based on different basis.

Remark 8 The methodology of derivation of energy-preserving scheme in the paper can be generalized to higher dimensional case. The mass matrix A and the stiffness matrix B can be easily obtained once a certain finite element is assigned. The only issue that should be carefully addressed is the computation of $F(U)$ in (13), since it involves a series of multiple integrals. In the following, we consider the two-dimensional case with rectangle domain $[x_L, x_R] \times [y_L, y_R]$. The domain is meshed with the spatial grid points $(x_i, y_j) = (x_L + (i-1)h, y_L + (j-1)h)$, $i = 1, 2, \ldots, N_x$, $j = 1, 2, \ldots, N_y$. A relatively simple choice of the basis functions would be $\{\phi_i(x)\phi_j(y),\ i = 1, 2, \ldots, N_x, j = 1, 2, \ldots, N_y\}$, where $\phi_i(x)$ is defined similarly as that shown in Fig. 1. In this case, after some tedious manipulation, the general entry of $F(U)$ can be simplified as follows.

$$\begin{aligned}
&\int_{x_L}^{x_R}\int_{y_L}^{y_R} \phi_i(x)\phi_j(y) \frac{V\left(\sum_{k=1}^{N_x}\sum_{l=1}^{N_y} w_{k,l}^{n+1}\phi_k(x)\phi_l(y)\right) - V\left(\sum_{k=1}^{N_x}\sum_{l=1}^{N_y} w_{k,l}^{n}\phi_k(x)\phi_l(y)\right)}{\sum_{k=1}^{N_x}\sum_{l=1}^{N_y} w_{k,l}^{n+1}\phi_k(x)\phi_l(y) - \sum_{k=1}^{N_x}\sum_{l=1}^{N_y} w_{k,l}^{n}\phi_k(x)\phi_l(y)} dxdy \\
&= h^2\int_0^1\int_0^1 \xi\eta \frac{V(\tilde{w}_1) - V(\tilde{w}_2)}{\tilde{w}_1 - \tilde{w}_2} d\xi d\eta + h^2\int_0^1\int_0^1 \xi(1-\eta)\frac{V(\tilde{w}_3) - V(\tilde{w}_4)}{\tilde{w}_3 - \tilde{w}_4} d\xi d\eta \\
&\quad + h^2\int_0^1\int_0^1 (1-\xi)\eta \frac{V(\tilde{w}_5) - V(F_6)}{\tilde{w}_5 - \tilde{w}_6} d\xi d\eta + h^2\int_0^1\int_0^1 (1-\xi)(1-\eta)\frac{V(\tilde{w}_7) - V(\tilde{w}_8)}{\tilde{w}_7 - \tilde{w}_8} d\xi d\eta
\end{aligned}$$

with

$$\tilde{w}_1 = \left((1-\xi)\left(w_{i-1,j-1}^{n+1}(1-\eta) + w_{i-1,j}^{n+1}\eta\right) + \xi\left(w_{i,j-1}^{n+1}(1-\eta) + w_{i,j}^{n+1}\eta\right)\right),$$
$$\tilde{w}_2 = \left((1-\xi)\left(w_{i-1,j-1}^{n}(1-\eta) + w_{i-1,j}^{n}\eta\right) + \xi\left(w_{i,j-1}^{n}(1-\eta) + w_{i,j}^{n}\eta\right)\right),$$

$$\tilde{w}_3 = \left((1-\xi)\left(w_{i-1,j}^{n+1}(1-\eta) + w_{i-1,j+1}^{n+1}\eta\right) + \xi\left(w_{i,j}^{n+1}(1-\eta) + w_{i,j+1}^{n+1}\eta\right)\right),$$
$$\tilde{w}_4 = \left((1-\xi)\left(w_{i-1,j}^{n}(1-\eta) + w_{i-1,j+1}^{n}\eta\right) + \xi\left(w_{i,j}^{n}(1-\eta) + w_{i,j+1}^{n}\eta\right)\right),$$
$$\tilde{w}_5 = \left((1-\xi)\left(w_{i,j-1}^{n+1}(1-\eta) + w_{i,j}^{n+1}\eta\right) + \xi\left(w_{i+1,j-1}^{n+1}(1-\eta) + w_{i+1,j}^{n+1}\eta\right)\right),$$
$$\tilde{w}_6 = \left((1-\xi)\left(w_{i,j-1}^{n}(1-\eta) + w_{i,j}^{n}\eta\right) + \xi\left(w_{i+1,j-1}^{n}(1-\eta) + w_{i+1,j}^{n}\eta\right)\right),$$
$$\tilde{w}_7 = \left((1-\xi)\left(w_{i,j}^{n+1}(1-\eta) + w_{i,j+1}^{n+1}\eta\right) + \xi\left(w_{i+1,j}^{n+1}(1-\eta) + w_{i+1,j+1}^{n+1}\eta\right)\right),$$
$$\tilde{w}_8 = \left((1-\xi)\left(w_{i,j}^{n}(1-\eta) + w_{i,j+1}^{n}\eta\right) + \xi\left(w_{i+1,j}^{n}(1-\eta) + w_{i+1,j+1}^{n}\eta\right)\right).$$

Similar to the one-dimensional case, these double integrals could be approximated by suitable two-dimensional quadrature formulae.

4 Numerical experiments

As discussed above, conservation laws play an important role in the theory of solitons. Therefore, in this section we pay attention to the following two Klein–Gordon equations and show the conservative property of the proposed new scheme.

Problem 1: single-soliton

We consider the nonlinear Klein–Gordon equation

$$\frac{\partial^2 u}{\partial t^2}(x,t) - a^2\frac{\partial^2 u}{\partial x^2}(x,t) + au(x,t) - bu^3(x,t) = 0, \tag{35}$$

on the region $(x,t) \in [-10,10] \times [0,10]$, with the initial conditions

$$u(x,0) = \sqrt{\frac{2a}{b}}\,\mathrm{sech}(\lambda x), \quad u_t(x,0) = c\lambda\sqrt{\frac{2a}{b}}\,\mathrm{sech}(\lambda x)\tanh(\lambda x),$$

in which $\lambda = \sqrt{\frac{a}{a^2-c^2}}$ and $a, b, a^2 - c^2 > 0$.

The exact solution is

$$u(x,t) = \sqrt{\frac{2a}{b}}\,\mathrm{sech}(\lambda(x-ct)). \tag{36}$$

The real parameter $\sqrt{2a/b}$ represents the amplitude of a soliton which travels with the velocity c. The problem can be found in [9,31], we choose $a = 0.3$, $b = 1$ and $c = 0.25$ similar to [9].

For the semi-discretisized system of this problem, we have

$$\begin{cases} F_1 = -\int_{x_1}^{x_2} \left(a\left(w_1\phi_1(x)+w_2\phi_2(x)\right)-b\left(w_1\phi_1(x)+w_2\phi_2(x)\right)^3\right)\phi_1(x)dx; \\ F_i = -\int_{x_{i-1}}^{x_i} \left(a\left(w_{i-1}\phi_{i-1}(x)+w_i\phi_i(x)\right)-b\left(w_{i-1}\phi_{i-1}(x)+w_i\phi_i(x)\right)^3\right)\phi_i(x)dx \\ \quad -\int_{x_i}^{x_{i+1}} \left(a\left(w_i\phi_i(x)+w_{i+1}\phi_{i+1}(x)\right)-b\left(w_i\phi_i(x)+w_{i+1}\phi_{i+1}(x)\right)^3\right)\phi_i(x)dx, \\ \quad i=2,\ldots,N-1; \\ F_N = -\int_{x_{N-1}}^{x_N} \left(a\left(w_{N-1}\phi_{N-1}(x)+w_N\phi_N(x)\right)\right. \\ \quad \left.-b\left(w_{N-1}\phi_{N-1}(x)+w_N\phi_N(x)\right)^3\right)\phi_N(x)dx, \end{cases} \tag{37}$$

and

$$\overline{V}(U)=\int_{x_L}^{x_R} V\left(\Phi(x)^{\mathsf{T}}U\right)dx$$

with $V(u)=\frac{a}{2}u^2-\frac{b}{4}u^4+0.15$. Therefore, when calculating the numerical energy, we can obtain

$$\begin{aligned} \overline{V}(U) &= \sum_{i=1}^{N-1}\int_{x_i}^{x_{i+1}} V(\phi_i(x)w_i^n+\phi_{i+1}(x)w_{i+1}^n)dx \\ &\overset{\xi=\frac{x-x_i}{h}}{=\!=\!=} \sum_{i=1}^{N-1}\int_0^1 V\left((1-\xi)w_i^n+\xi w_{i+1}^n\right)d\xi \\ &= (N-1)\times 0.15+\sum_{i=1}^{N-1}\frac{\frac{a}{6}{w_{i+1}^n}^3-\frac{b}{20}{w_{i+1}^n}^5-\frac{a}{6}{w_i^n}^3+\frac{b}{20}{w_i^n}^5}{w_{i+1}^n-w_i^n}. \end{aligned}$$

In the experiment we choose the stepsizes $h=0.04$, $\tau=0.01$. First, by approximating the integral with two-point Gauss–Legendre's rule, we apply the numerical scheme derived in this paper to the problem. The tolerance 10^{-11} is chosen for solving the nonlinear algebraic equations by the fixed-point iteration method. Notice that h, τ is chosen as $h=0.04$, $\tau=0.01$ to ensure that the fixed-point iteration is convergent at every time step. The numerical solution and the numerical error between the numerical solution and the exact solution are shown in Figs. 2 and 3.

Then, we show the conservative property of the scheme with two-point Gauss–Legendre's rule and four-point Gauss–Legendre's rule, in Figs. 4 and 5 respectively. We plot the relative energy error $\left|\tilde{E}(t_n)-E(t_0)\right|/E(t_0)$ (from a continuous PDE to a full discrete system) and the relative semidiscrete energy error $\left|\tilde{E}(t_n)-\tilde{E}(t_0)\right|/\tilde{E}(t_0)$ (from semidiscrete ODEs to full discrete system).

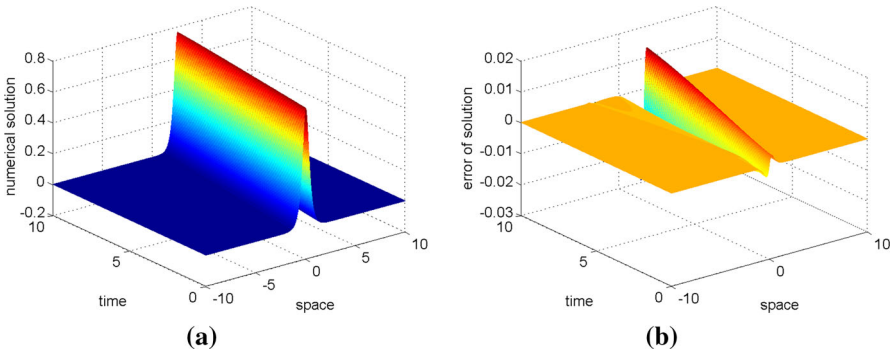

Fig. 2 **a** Motion of the single-soliton by the scheme with two-point Gauss–Legendre's rule. **b** Error between numerical solution and the exact solution

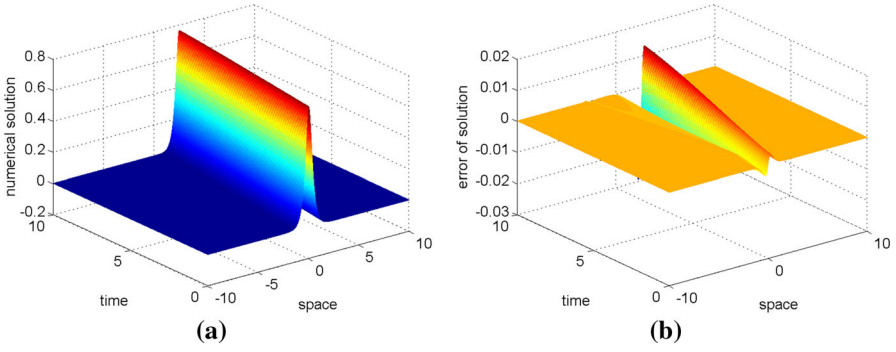

Fig. 3 **a** Motion of the single-soliton by the scheme with four-point Gauss–Legendre's rule. **b** Error between numerical solution and the exact solution

It can be observed from Figs. 2b and 3b that the numerical solution errors for both schemes with two-point and four-point Gauss–Legendre's rules grows linearly as time increases. The errors between two cases are comparative. For the energy conservation, the two errors of full discrete energy are almost the same. However, for the semidiscrete energy conservation, in the case of two-point Gauss–Legendre's rule, the error grows with time, whereas in the case of four-point Gauss–Legendre's rule, the error is at the level of round-off. Thus the precision of the quadrature for the integrations in the scheme have more influence on the precision of numerical energy than that of numerical solution. The reason is that the energy is the accumulation of the solution in all nodal points.

For this problem, $E(t_0) = 3.118904086633647$ is obtained by using the initial conditions and implementing 'NIntegrate' of the software 'Mathematica 5' with options 'WorkingPrecision→ 50' and 'PrecisionGoal→ 16'.

Problem 2: breather soliton

Among the important equations that possess an infinite number of conservation laws is the sine-Gordon equation, which can be found in many applications (e.g., [32,33]). The conservation of energy is an essential property in an elastic collision of two solitons. However, many existing numerical algorithms fail to preserve the system

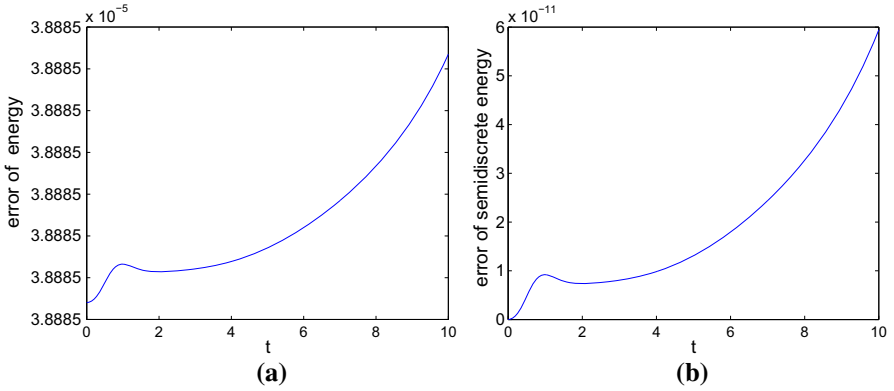

Fig. 4 Conservative property of the scheme with two-point Gauss–Legendre's rule. **a** $\left|\tilde{E}(t_n) - E(t_0)\right| / E(t_0)$. **b** $\left|\tilde{E}(t_n) - \tilde{E}(t_0)\right| / \tilde{E}(t_0)$

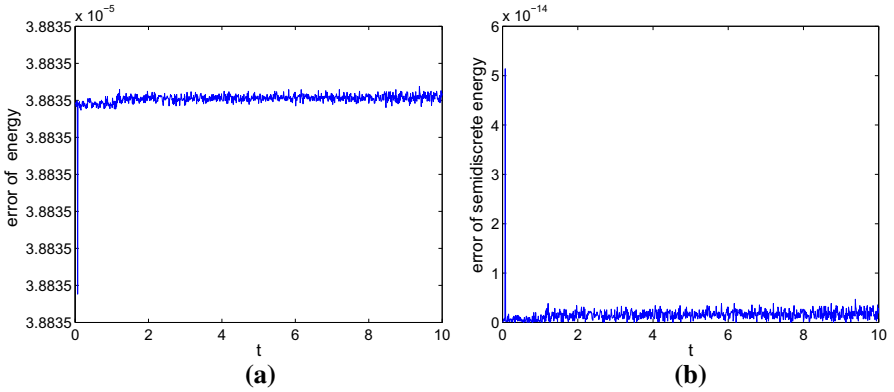

Fig. 5 Conservative property of the scheme with four-point Gauss–Legendre's rule. **a** $\left|\tilde{E}(t_n) - E(t_0)\right| / E(t_0)$. **b** $\left|\tilde{E}(t_n) - \tilde{E}(t_0)\right| / \tilde{E}(t_0)$

energy. The problem is given by the following equation

$$\frac{\partial^2 u}{\partial t^2}(x,t) - \frac{\partial^2 u}{\partial x^2}(x,t) = -\sin(u(x,t)), \quad (x,t) \in [-10,10] \times [-20,20]. \tag{38}$$

The initial conditions are

$$u(x,-20) = -4\arctan\left(c^{-1}\operatorname{sech}\left(\frac{x}{\sqrt{1+c^2}}\right)\sin\left(\frac{20c}{\sqrt{1+c^2}}\right)\right)$$

$$u_t(x,-20) = \frac{4\cos\left(\frac{20c}{\sqrt{1+c^2}}\right)\operatorname{sech}\left(\frac{x}{\sqrt{1+c^2}}\right)}{\sqrt{1+c^2}\left(1+\frac{\operatorname{sech}^2\left(\frac{x}{\sqrt{1+c^2}}\right)\sin^2\left(\frac{20c}{\sqrt{1+c^2}}\right)}{c^2}\right)},$$

and the exact solution of (38) is given by

$$u(x,t) = 4\arctan\left(c^{-1}\sin(ct/\sqrt{1+c^2})\mathrm{sech}(x/\sqrt{1+c^2})\right).$$

For the semi-discretisized system of this problem, we have

$$\begin{cases} F_1 = -\displaystyle\int_{x_1}^{x_2} \sin\left(w_1\phi_1(x) + w_2\phi_2(x)\right)\phi_1(x)dx; \\ F_i = -\displaystyle\int_{x_{i-1}}^{x_i} \sin\left(w_{i-1}\phi_{i-1}(x) + w_i\phi_i(x)\right)\phi_i(x)dx \\ \qquad -\displaystyle\int_{x_i}^{x_{i+1}} \sin\left(w_i\phi_i(x) + w_{i+1}\phi_{i+1}(x)\right)\phi_i(x)dx,\ i = 2,\ldots,N-1; \\ F_N = -\displaystyle\int_{x_{N-1}}^{x_N} \sin\left(w_{N-1}\phi_{N-1}(x) + w_N\phi_N(x)\right)\phi_N(x)dx, \end{cases} \tag{39}$$

and

$$\overline{V}(U) = \int_{x_L}^{x_R} V\left(\Phi(x)^{\mathsf{T}}U\right)dx$$

with $V(u) = 1 - \cos(u)$. Similarly, for this problem we can also obtain

$$\overline{V}(U) = (N-1) - \sum_{i=1}^{N-1} \frac{\sin(w_{i+1}^n) - \sin(w_i^n)}{w_{i+1}^n - w_i^n}.$$

This problem is known as the breather solution of the sine-Gordon equation and represent a pulse-type structure of a soliton. The parameter c is the velocity and in the experiment we choose $c = 0.5$ and the stepsizes $h = 0.04$, $\tau = 0.01$. By approximating the integral with two-point Gauss–Legendre's rule, we apply the numerical scheme to this problem. The tolerance 10^{-12} is chosen for solving the nonlinear algebraic equations by the fixed-point iteration method. The numerical solution and the numerical error between the numerical solution and the exact solution are shown in Figs. 6 and 7. The conservative property of the scheme with two-point Gauss–Legendre's rule and four-point Gauss–Legendre's rule are shown in Figs. 8 and 9, respectively.

It can be observed from Figs. 6b and 7b that the numerical solution errors for both schemes increase in a oscillatory way and are comparative. For the energy conservation, the two errors of full discrete energy are almost the same. However, for the semidiscrete energy conservation, in the case of two-point Gauss–Legendre's rule, the error oscillates periodically at an order of magnitude 10^{-10}, whereas in the case of four-point Gauss–Legendre's rule, the error is at the order of magnitude 10^{-13} but grows slowly and linearly with time.

For this problem, $E(t_0) = 14.3108337357790822$ is obtained in the same way as Problem 1.

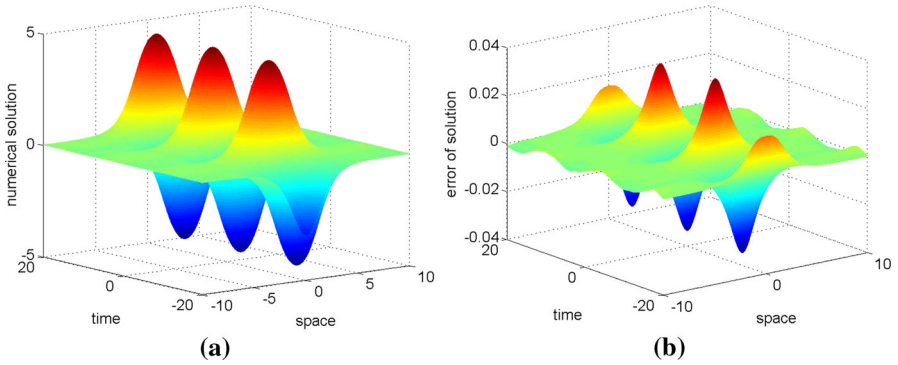

Fig. 6 **a** Motion of the breather soliton by the scheme with two-point Gauss–Legendre's rule. **b** Error between numerical solution and the exact solution

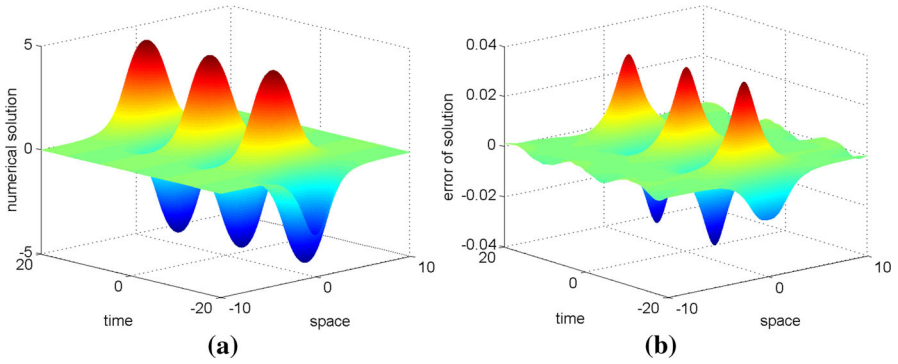

Fig. 7 **a** Motion of the breather soliton by the scheme with four-point Gauss–Legendre's rule. **b** Error between numerical solution and the exact solution

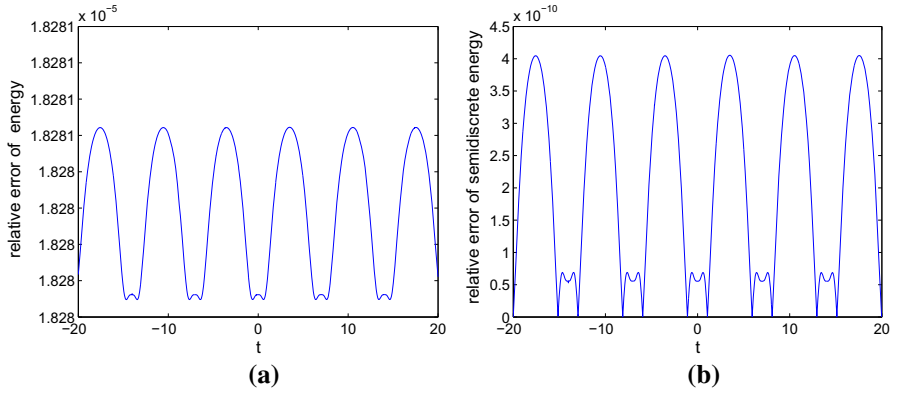

Fig. 8 Conservative property of the scheme with two-point Gauss–Legendre's rule. **a** $\left|\tilde{E}(t_n) - E(t_0)\right| / E(t_0)$. **b** $\left|\tilde{E}(t_n) - \tilde{E}(t_0)\right| / \tilde{E}(t_0)$

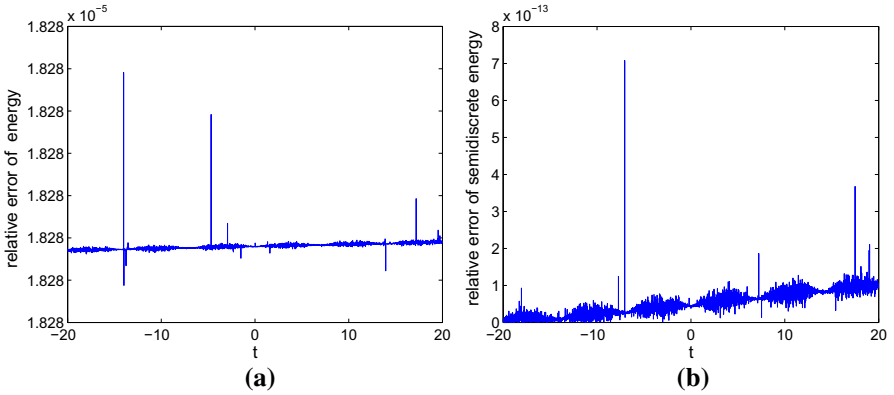

Fig. 9 Conservative property of the scheme with four-point Gauss–Legendre's rule. **a** $\left|\tilde{E}(t_n) - E(t_0)\right| / E(t_0)$. **b** $\left|\tilde{E}(t_n) - \tilde{E}(t_0)\right| / \tilde{E}(t_0)$

5 Conclusions

In this paper, incorporating FEM with the AVF approach, we proposed and analyzed a new energy-preserving scheme for nonlinear Hamiltonian wave equations. In the study, as the first step, we considered the weak formulation and presented the finite element formulation for the framework of the scheme. Moreover, the stability of the semi-discrete finite element scheme was analyzed. For time discretization, the AVF approach is used to preserve the semidiscrete energy obtained by the first step. The perfect combination of FEM and AVF approach results in a new and efficient numerical scheme for nonlinear Hamiltonian wave equations. As important test problems, numerical experiments on a single-soliton problem and a sine-Gordon equation were implemented and the numerical results show the remarkable conservative property of the proposed numerical scheme.

References

1. Reich, S.: Multi-symplectic Runge–Kutta collocation methods for Hamiltonian wave equations. J. Comput. Phys. **157**, 473–499 (2000)
2. Ge, Z., Marsden, J.E.: Lie-Poisson Hamilton–Jacobi theory and Lie-Poisson integrators. Phys. Lett. A **133**, 134–139 (1988)
3. Wazwaz, A.M.: New travelling wave solutions to the Boussinesq and the Klein–Gordon equations. Commun. Nonlinear Sci. Numer. Simul. **13**, 889–901 (2008)
4. Dodd, R.K., Eilbeck, I.C., Gibbon, J.D., Morris, H.C.: Solitons and Nonlinear Wave Equations. Academic, London (1982)
5. Biswas, A.: Soliton perturbation theory for phi-four model and nonlinear Klein–Gordon equations. Commun. Nonlinear Sci. Numer. Simul. **14**, 3239–3249 (2009)
6. Shakeri, F., Dehghan, M.: Numerical solution of the Klein–Gordon equation via He's variational iteration method. Nonlinear Dyn. **51**, 89–97 (2008)
7. Dehghan, M.: Finite difference procedures for solving a problem arising in modeling and design of certain optoelectronic devices. Math. Comput. Simul. **71**, 16–30 (2006)

8. Dehghan, M., Mirezaei, D.: Numerical solution to the unsteady two-dimensional Schrodinger equation using meshless local boundary integral equation method. Int. J. Numer. Methods Eng. **76**, 501–520 (2008)
9. Bratsos, A.G.: On the numerical solution of the Klein–Gordon equation. Numer. Methods Partial Differ. Equ. **25**, 939–951 (2009)
10. Budd, C.J., Piggot, M.D.: Geometric Integration and Its Applications, Handbook of Numerical Analysis, vol. XI. North-Holland, Amsterdam (2003)
11. Li, S., Vu-Quoc, L.: Finite difference calculus invariant structure of a class of algorithms for the nonlinear Klein–Gordon equation. SIAM J. Numer. Anal. **32**, 1839–1875 (1995)
12. Ide, T., Okada, M.: Numerical simulation for a nonlinear partial differential equation with variable coefficients by means of the discrete variational derivative method. J. Comput. Appl. Math. **194**, 425–459 (2006)
13. Celledoni, E., Grimm, V., McLachlan, R.I., McLaren, D.I., O'Neale, D., Owren, B., Quispel, G.R.W.: Preserving energy resp. dissipation in numerical PDEs using the "average vector field" method. J. Comput. Phys. **231**, 6770–6789 (2012)
14. Chabassier, J., Joly, P.: Energy preserving schemes for nonlinear Hamiltonian systems of wave equations: application to the vibrating piano string. Comput. Methods Appl. Mech. Eng. **199**, 2779–2795 (2010)
15. Schiesser, W.: The numerical methods of liness: integration of partial differential equation. Academic Press, San Diego (1991)
16. Quispel, G.R.W., McLaren, D.I.: A new class of energy-preserving numerical integration methods. J. Phys. A. **41**, 045206 (2008)
17. Shampine, L.F.: Conservation laws and the numerical solution of ODEs. Math. Appl. B **12**, 1287–1296 (1986)
18. McLachlan, R.I., Quispel, G.R.W., Robidoux, N.: Geometric integration using discrete gradients. Philos. Trans. R. Soc. A **357**, 1021–1045 (1999)
19. Iserles, A., Zanna, A.: Preserving algebraic invariants with Runge–Kutta methods. J. Comput. Appl. Math. **125**, 69–81 (2000)
20. Iserles, A., Quispel, G.R.W., Tse, P.S.P.: B-series methods cannot be volume-preserving. BIT Numer. Math. **47**, 351–378 (2007)
21. Hairer, E., McLachlan, R.I., Skeel, R.D.: On energy conservation of the simplified Takahashi-Imada method. Math. Model. Numer. Anal. **43**, 631–644 (2009)
22. McLachlan, R.I., Quispel, G.R.W., Tse, P.S.P.: Linearization-preserving selfadjoint and symplectic integrators. BIT Numer. Math. **49**, 177–197 (2009)
23. Wu, X., Wang, B., Shi, W.: Efficient energy-preserving integrators for oscillatory Hamiltonian systems. J. Comput. Phys. **235**, 587–605 (2013)
24. Liu, K., Shi, W., Wu, X.: An extended discrete gradient formula for oscillatory Hamiltonian systems. J. Phys. A Math. Theor. **46**(16520), 3 (2013)
25. Wang, B., Wu, X., Meng, F.: Trigonometric collocation methods based on Lagrange basis polynomials for multi-frequency oscillatory second order differential equations. J. Comput. Appl. Math. **313**, 185–201 (2017)
26. Wang, B., Yang, H., Meng, F.: Sixth order symplectic and symmetric explicit ERKN schemes for solving multi frequency oscillatory nonlinear Hamiltonian equations. Calcolo **54**, 117–140 (2017)
27. Wang, B., Iserles, A., Wu, X.: Arbitrary order trigonometric Fourier collocation methods for second-order ODEs. Found. Comput. Math. **16**, 151–181 (2016)
28. Lions, J., Magenes, E.: Non-homogeneous Boundary Value Problems and Applications, vol. I. Springer, New York (1972)
29. Butcher, J.C.: Numerical Analysis of Ordinary Differential Equations, 2nd edn. Wiley, New York (2008)
30. Lambert, J.D., Watson, I.A.: Symmetric multistip methods for periodic initial value problems. J. Inst. Math. Appl. **18**(189–20), 2 (1976)
31. Dehghan, M., Mohebbi, A., Asgari, Z.: Fourth-order compact solution of the nonlinear Klein–Gordon equation. Numer. Algor. **52**, 523–540 (2009)
32. Bratsos, A.G.: A numerical method for the one-dimentional sine-Gordon equation. Numer. Mehods Partial Differ. Equ. **24**(833–84), 4 (2008)
33. Mohebbi, A., Dehghan, M.: High-order solution of one-dimensional sine-Gordon equation using compact finite difference and DIRKN methods. Math. Comput. Model. **51**, 537–549 (2010)